ACS Energy LETTERS

http://pubs.acs.org/journal/aelccp

CO_2 Reduction to Higher Hydrocarbons by Plasma Discharge in Carbonated Water

Sisi Yang, Bofan Zhao, Indu A. Aravind, Yu Wang, Boxin Zhang, Sizhe Weng, Zhi Cai, Ruoxi Li, Ali Zarei Baygi, Adam Smith, Martin A. Gundersen, and Stephen B. Cronin*

Cite This: *ACS Energy Lett.* 2021, 6, 3924–3930

Read Online

ACCESS | Metrics & More | Article Recommendations | Supporting Information

ABSTRACT: By discharging nanosecond high-voltage pulses in CO_2-saturated water, we observe CO_2 reduction to higher-order hydrocarbons, including acetic acid, formic acid, and oxalate. Here, the plasma emission spectra exhibit Swan bands, which correspond to C_2 species, indicating that in addition to reducing CO_2, C_2-species are formed, which presents the possibility of converting a notorious greenhouse gas into liquid (*i.e.*, dense) hydrocarbon fuels. In order to characterize various hydrocarbon products formed in this process, cryogenic NMR spectroscopy and liquid ion chromatography are performed *ex situ*. Here, we observe clear peaks corresponding to formic acid (CH_2O_2) and acetic acid (CH_3COOH). We have also observed the presence of formate (HCO_2^-), acetate ($C_2H_3O_2^-$), and oxalate ($C_2O_4^{2-}$) using liquid ion chromatography. Plasma emission spectroscopy exhibits spectral signatures associated with atomic hydrogen and atomic oxygen due to the plasma discharge in water, which facilitate (and compete with) the CO_2-to-hydrocarbon conversion.

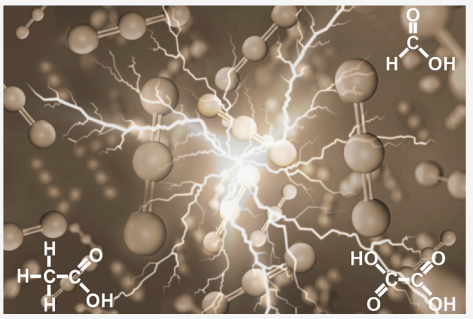

With increasing levels of greenhouse gases in our atmosphere, CO_2 reduction processes are of broad interest because of their ability to mitigate global warming. Many research groups (including our own) have focused on electrochemical and photoelectrochemical CO_2 reduction, involving various metal electrodes, molecule catalysts, and plasmon-enhanced approaches.[1−15] The reduction of CO_2 with H_2O to various hydrocarbons is a complex reaction system requiring up to 8 electrons and many intermediate species, some of which have extremely high energy barriers. The mechanism for electrochemical CO_2 reduction was first proposed by Bockris *et al.*[16−18] The high overpotential required for this reaction was attributed to the formation of the $(CO_2)^-$ intermediate, $CO_2 + e^- \rightarrow (CO_2)^-$, which is the rate-limiting step of CO_2 reduction. The highly energetic species provided by the plasma (*i.e.*, nonequilibrium approach) provide a strategy for overcoming the reaction barrier associated with the $(CO_2)^-$ reaction intermediate. Dielectric barrier discharge has been reported for conversion of carbon dioxide to syngas and hydrocarbons at atmosphere pressure with or without catalyst.[19−21] Heijkers *et al.*, Masaharu *et al.*, and Mitsingas *et al.* reported the decomposition of CO_2 by microwave plasma in carrier gases of N_2, Ar, or He.[22−24] Pulsed plasmas have also been used to drive gas-phase CO_2 reduction reactions and subsequent conversion to hydrocarbon fuels (syngas).[25−28]

While there have been many papers reporting CO_2 reduction to higher-order hydrocarbons in the gas phase,[29−35] to our knowledge few have shown CO_2 reduction in carbonated water by plasma discharge. Rumbach *et al.* showed that CO_2 can be reduced in an aqueous medium using a plasma-based electrode to produce oxalate and formate.[36] In their work, the plasma discharge was generated in the gas phase (above liquid) and highly energetic electrons were injected into the solution, thus producing solvated electrons. Generating a plasma discharge in aqueous solutions requires voltages significantly higher than that in the gas phase because of the relatively high dielectric strength of the aqueous medium. Common approaches to lowering the discharge threshold include using a needle electrode, a gas diffuser, or pressurization to create bubbles, enabling the discharge to be initiated within a small bubble on the electrode surface and then propagate into the aqueous phase.[37−45]

In the work presented here, we demonstrate CO_2 reduction to higher-order hydrocarbons by discharging a nanosecond pulsed plasma in carbonated (*i.e.*, CO_2-satuarated) aqueous

Received: August 9, 2021
Accepted: October 4, 2021

solution. Here, the carbonated water gives rise to small bubbles which lower the voltage needed to generate the plasma and also provides a relatively high concentration of CO_2 in the aqueous solution.

In the work presented here, the transient pulsed plasma is produced on a glass slide-based reactor with a high-voltage pulse generator (Model 30X, Transient Plasma Systems, Inc.), which produces pulses with peak voltages up to 30 kV, pulse rise times of 5−10 ns, and repetition rates up to 2 kHz. A typical waveform is shown in Figure 1b. Figure S1 in the Supporting Information shows a plot of our waveform characteristics over several cycles, in which the short nanosecond pulses are repeated at a rate of 1 kHz, giving rise to a duty cycle of approximately 1:10^5. The *in situ* plasma emission spectra are taken with an *inVia* Raman microspectrometer (Renishaw, Inc.). The cryogenic NMR spectroscopy and liquid ion chromatography (Dionex, ICS-2000) are performed *ex situ* before and after 30 min plasma discharges in 10 mL of carbonated solution. The Dionex Ion Chromatography System (ICS-2000, Thermo Fisher Scientific, Sunnyvale, CA) is equipped with a refrigerated autosampler and has a detection limit of 0.1 mg/L for the tested compounds.

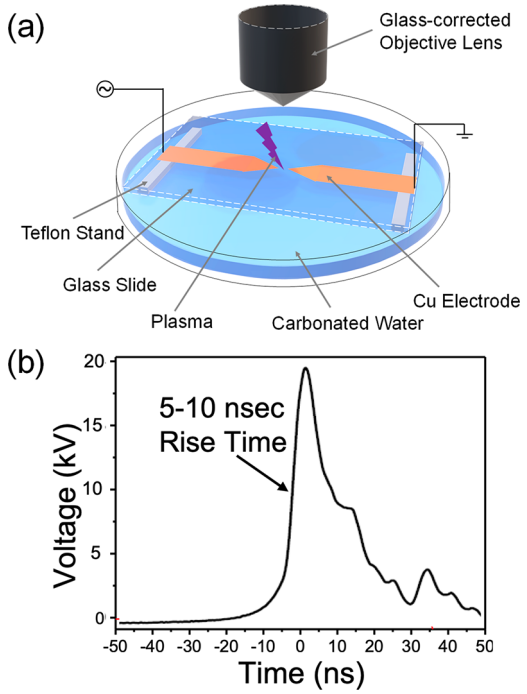

Figure 1. (a) Schematic diagram of the experimental setup used to take *in situ* plasma emission spectra. (b) Typical output characteristics of nanosecond high-voltage pulse generator.

Figure 1a shows a schematic diagram of our experimental setup for observing plasma emission spectroscopy. Here, two copper tape electrodes, separated by a 5 mm gap, are attached to the bottom side of a 1 mm-thick glass slide, and immersed in the carbonated water electrolyte, while the top surface of the glass slide remains in air. This geometry enables plasma emission spectra to be taken efficiently using a glass-corrected objective lens.Figure 2 shows several photographs of the plasma discharge using copper tape electrodes deposited on a glass slide in DI water (deionized water) and CO_2-satuarated DI water at 13 kV (Figure 2a) and 28 kV (Figure 2b). In DI water, 28 kV pulses are needed in order to generate a plasma, which is much higher than the voltages required to create a plasma in the gas phase (~5 kV)[46,47] because of the relatively high dielectric strength of the aqueous medium, which has a breakdown field 5−6 times higher than that of air. The copper electrodes are patterned with sharp tips to provide additional field enhancement to help initiate the plasma. In carbonated water, we can achieve plasma discharge at 13 kV because of the presence of bubbles. The aqueous solution can potentially provide a higher density of reactants than gas-phase reactions. In our measurement, the carbonated water was produced at room temperature (25 °C) using a SodaStream water-carbonator, which is capable of carbonating the water at approximately 20 PSI, from which we estimate the initial amount of CO_2 in solution to be around 2 g/L.[48] Carbon dioxide dissolves in water at 0.2−1.0% concentration (1.45−3.0 g/L), which creates carbonic acid (H_2CO_3).[49−52] However,

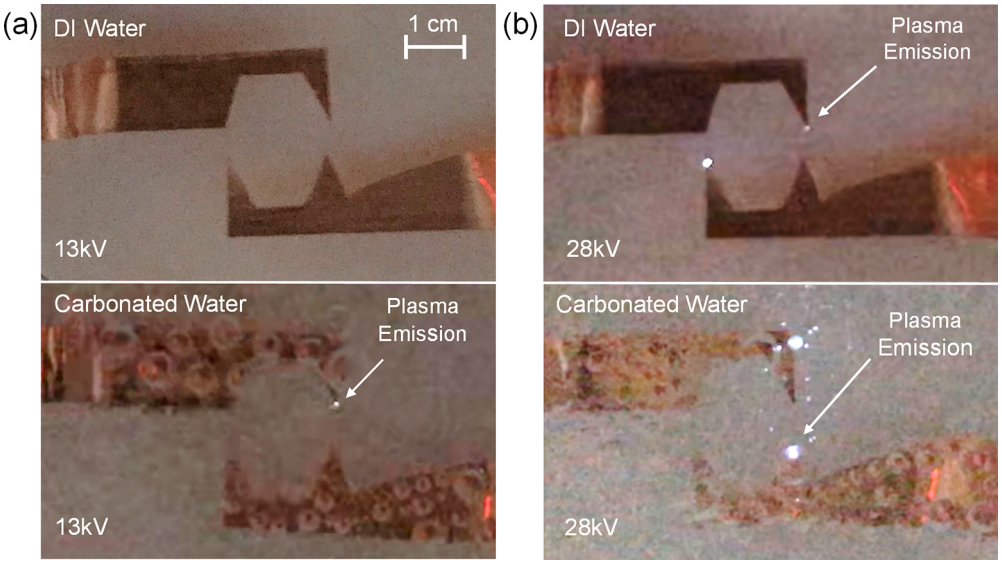

Figure 2. Plasma emission generated with copper tape electrodes in deionized (DI) water and carbonated water at (a) 13 kV and (b) 28 kV.

https://doi.org/10.1021/acsenergylett.1c01666
ACS Energy Lett. 2021, 6, 3924−3930

the plasma discharge is likely initiated within bubbles of gaseous CO_2, because it is easier to achieve a plasma discharge in gas than in liquid. That is, the reported dielectric strength of air is 22× less than that of water. We believe that it is these CO_2-rich pockets that enable C_2 formation, in the gas-phase plasma, liquid phase, or some interaction between the gas and liquid phases.[24,53−57]

Figure 3 shows plasma emission spectra of our transient pulsed plasma obtained in a CO_2-saturated aqueous environment taken with a high numerical aperture objective lens, as illustrated in Figure 1a. Here, we observe several sets of Swan bands, which correspond to C_2 (diatomic carbon) species.[58,59] For example, C_2(1,0), C_2(0,0), and C_2(0,1) correspond to different vibrational and rotational states of this diatomic species. This indicates that, in addition to reducing CO_2 (*i.e.*, a high barrier reaction), C_2-species are formed, which may subsequently convert to acetate ($C_2H_3O_2^-$) and oxalate ($C_2O_4^{2-}$), as detected by liquid ion chromatography (see Figure 4). While copper is a well-known CO_2 electrocatalyst,[1,6,60−63] we have conducted additional experiments with aluminum electrodes instead of copper. Here, we found comparable C_2 species as plotted in the spectra shown in Figure S2. Therefore, we do not believe that the copper electrodes themselves are catalytically activating the CO_2 independent of the plasma.

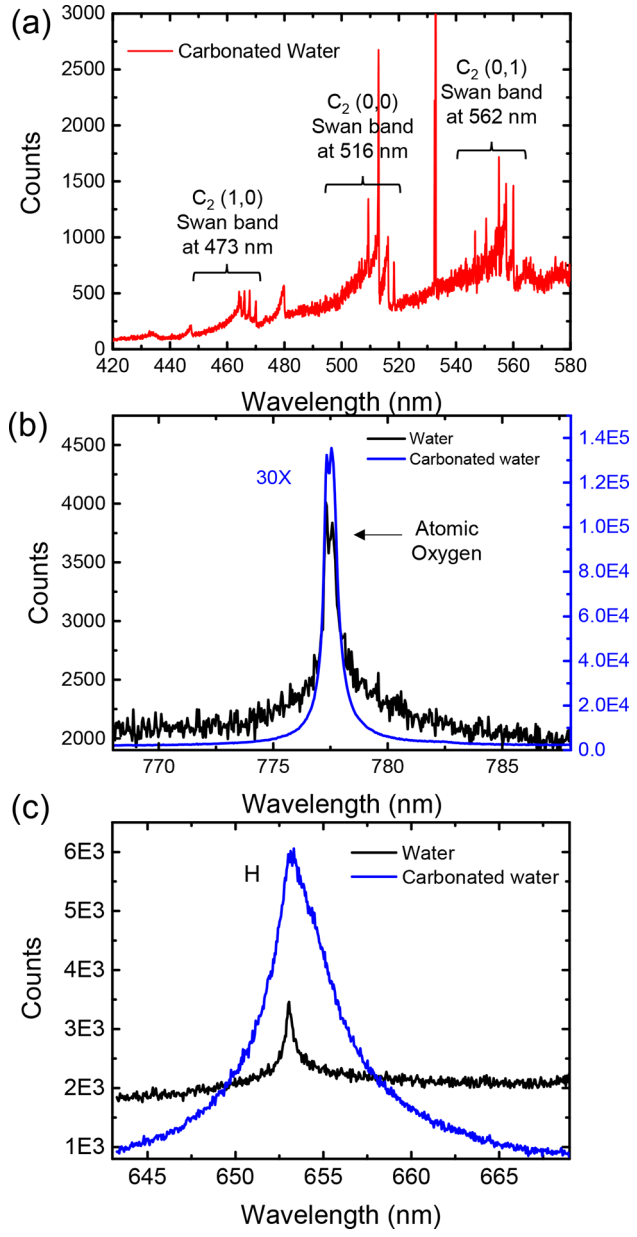

Figure 3. Plasma emission spectra of (a) C_2 species, (b) atomic O, and (c) H radicals observed in DI water and carbonated water with 15 kV pulses at the repetition rate of 400 Hz.

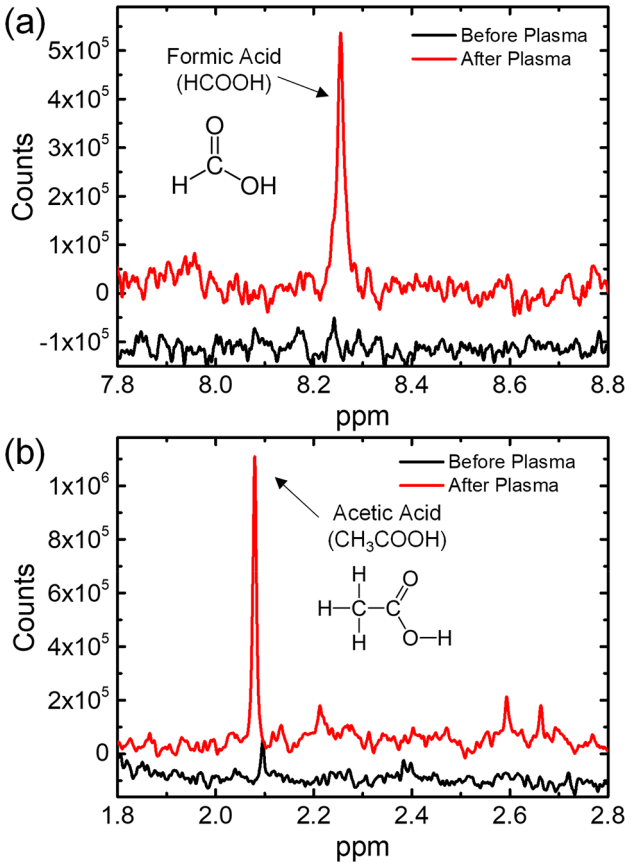

Figure 4. Cryogenic ^{1}H NMR spectra taken before and after 30 min plasma discharge in CO_2-saturated water of (a) formic acid and (b) acetic acid.

From a pulsed discharge in water, we also observe features in the emission spectra associated with the H and O radicals, which correspond to highly chemically reactive species.[64−68] One of the main challenges in producing hydrocarbons using a plasma is that the atomic oxygen rapidly drives the back reaction of carbon to CO and CO_2. Panels b and c of Figure 3 show the plasma emission spectra corresponding to atomic oxygen and hydrogen. Here, both the H and O radicals are more easily generated in carbonated water than in DI water because of the presence of bubbles which assist in the plasma discharge process, thereby generating a higher-density plasma under the same voltage conditions. As mentioned above, the formation of CO_2 bubbles gives rise to a lower threshold for plasma discharge than in DI water. This finding is consistent with previous papers on plasma discharge in water, most of which provide some strategy for creating bubbles and thus lowering the plasma discharge threshold.[37−45] Dobrynin and co-workers investigated the initiation stage of nanosecond

https://doi.org/10.1021/acsenergylett.1c01666
ACS Energy Lett. 2021, 6, 3924−3930

breakdown in liquid, which revealed the appearance of discontinuities in the liquid (cavitation) under the influence of electrostriction forces.[69] It is possible that this cavitation effect is more pronounced in the carbonated water electrolyte; however, these experiments could not be performed with our existing experimental setup.

In order to quantify the hydrocarbons produced by the plasma discharge in carbonated water, we performed cryogenic NMR spectroscopy of various products in water (*i.e.*, hydrocarbons) and liquid ion chromatography *ex situ*. Figure 4 shows cryogenic NMR spectra taken before and after plasma discharge in CO_2-saturated water. Here, we observe clear peaks corresponding to formic acid and acetic acid, which corresponds to a C_2-hydrocarbon species. We have also observed the presence of oxalates (*i.e.*, $C_2O_4^{2-}$) using liquid ion chromatography, as shown in Figure S4, which also correspond to C_2 species.

One possible reaction pathway takes place *via* hot electrons generated in the bubbles, which are subsequently injected into the aqueous solution forming solvated electrons, which have an extremely high reduction potential.[70,71] This reaction can potentially follow the pathway $CO_2 + e^- \rightarrow CO_2^-$ and then $CO_2^- + CO_2^- \rightarrow (CO_2^-)_2$ for oxalate and $CO_2^- + H^+ + e^- \rightarrow HCOO^-$ for formate.[36,72−75] Mota-Lima reported a theoretical overview of plasma/liquid interface as a platform for highly efficient CO_2 electroreduction to oxalate, in which the carboxyl radical anion (CO_2^-(aq)) plays an important role.[75] Here, the one-electron reduction to CO_2^- represents a high-barrier intermediate that is enabled by the high-energy electrons in the plasma and subsequent generation of solvated electrons.[36] This is essentially homogeneous chemistry in the aqueous phase driven by solvated electrons, which have an extremely low (*i.e.*, strongly) reducing potential (−2.87 V vs SHE or only 1.41 eV below vacuum). These solvated electrons, while difficult to form, have been used to drive difficult reactions such as ammonia formation, which transforms N_2 and water to NH_3 without a catalyst surface, as well as CO_2 reduction to CO.[70,71,76,77]

While it is possible that CO_2 reduction is induced by the formation of solvated electrons reported previously by Rumbach *et al.*,[36,71] the lifetime and penetration depth of these solvated electrons are quite small. It is, therefore, more likely that the reaction occurs in the gas phase (*i.e.*, in the bubbles),[25−28] where the CO_2 in the liquid phase continuously supplements the gas phase to ensure the continued progress of the reaction. The gas-phase reaction (in the bubble) can involve only CO_2, H radicals, O radicals, and H_2O. We have detected H_2 and CO by GC measurements (see Figure S3), which could serve as possible reaction intermediates. In this case, this process involves mixed phases: liquid, gas, and plasma. However, further studies would be needed in order to establish the precise proportion of these reactions that occur in the liquid and gas phases.

The production of acetic acid is especially interesting, as it has not been observed before and likely has a more complex reaction pathway than either formate or oxalate. While a detailed pathway for this reaction is not currently understood, two possible reaction pathways for acetic acid include the following:

(1) *Via* formate

$$HCOO^- + 5H^+ + 4e^- \rightarrow CH_3OH + H_2O$$

$$HCOO^- + CH_3OH + H^+ \rightarrow CH_3COOH + H_2O$$

$$(2HCOO^- + 6H^+ + 4e^- \rightarrow CH_3COOH + H_2O)$$

(2) *Via* oxalate

$$C_2O_4^{2-} + 8H^+ + 6e^- \rightarrow CH_3COOH + 2H_2O$$

Another possible mechanism was reported by Genovese *et al.* for C−C bond formation in the electrocatalytic reduction of CO_2 to acetic acid *via* the reaction of CO_2^- with surface adsorbed $-CH_3$ species.[78]

In this work, the formic acid and acetic acid yields are estimated to be 2.2×10^{-3} and 4.4×10^{-4} mol/L, respectively, based on cryogenic ^{1}H NMR spectroscopy with respect to a known amount of methanol (CH_3OH). The voltage and current waveforms (vs time) are plotted in Figure S6, which indicate an energy per pulse of 18.6 mJ. While the plasma density depends on many factors, including electrode geometry and dielectric medium, we estimate the efficiency of formic acid and acetic acid production to be 1.6×10^{-9} moles and 3.3×10^{-10} moles per Joule of energy based on the energy per pulse multiplied by the pulse repetition rate. While previous work on plasma-based CO_2 conversion carried out in the gas is typically reported in % CO_2 conversion efficiencies (*e.g.*, 5−35% energy efficiencies[31,79] or 10% faradaic efficiency[36]), no values in mol/Joule have been put forth for plasma discharge in an aqueous electrolyte. Assuming the formic acid and acetic acid production proceed in the gas phase, on the basis of the reaction enthalpy of the overall reactions $CO_2 + H_2O \rightarrow HCOOH + 1/2\ O_2$ (ΔH = 243 kJ/mol) and $2CO_2 + 2H_2O \rightarrow CH_3COOH + 2O_2$ (ΔH = 875 kJ/mol), we can estimate their energy efficiency to be around 1×10^{-7} mol/J for formic acid and 1×10^{-8} mol/J for acetic acid, which is 2 orders of magnitude larger than our results.

It should be noted that our current approach is far from optimized, and we believe several orders of magnitude improvement can be achieved by improving the electrode geometry, introducing catalytically active surfaces, and controlling the local electrode environment/potential. While discharging a plasma in water is particularly difficult, this provides a unique environment in which the ion concentrations can be varied by 14 orders of magnitude (*e.g.*, pH 0−14) (unlike gas-phase reactions), ultimately enabling us to better control reaction rates and selectivity. Upon introducing a catalytically active surface (*e.g.*, NiO), this CO_2 reduction reaction can be driven more efficiently.[34,35] It is interesting to note that the C_2 swan bands presented in Figure S2 are roughly a factor or 2 less intense than those obtained with Cu, plotted in Figure 3a. However, because of the inherent fluctuations in this water-based discharge, it is very hard to compare intensities. Lastly, by implementing electrode geometries that provide electric field enhancement, significant improvements in the overall efficiency can be achieved. For example, the active area over which the plasma is discharged in this work is limited to several square micrometers. Using a transmission line geometry, much larger areas of approximately square millimeters can be achieved.[80−83] Further approaches to improving efficiency include employing an active means of

https://doi.org/10.1021/acsenergylett.1c01666
ACS Energy Lett. 2021, 6, 3924−3930

separating the products from the reactants (*e.g.*, azeotropic distillation), which enable the accumulation of a significant amount of product while minimizing destructive back reactions.

We have demonstrated CO_2 reduction to C_1 and C_2 hydrocarbons by discharging nanosecond high-voltage pulses in carbonated (*i.e.*, CO_2-saturated) water. After discharging plasma, we observe the formation of acetic acid, formic acid, and oxalate through the complex interaction between liquid, gas, and plasma phases. Swan bands are exhibited in the plasma emission spectra, confirming the formation of C_2 (diatomic carbon radical) species. A substantially lower threshold voltage is needed to generate a plasma in carbonated water than in DI water because of bubbles formed on the electrode surface. Cryogenic NMR spectroscopy reveals clear peaks corresponding to formic acid (CH_2O_2) and acetic acid (CH_3COOH), and liquid ion chromatography shows the presence of oxalates (*i.e.*, $C_2O_4^{2-}$) after discharging plasma in carbonated water. Electrodes mounted on a glass slide form a submerged planar surface discharge that enables plasma emission spectra to be obtained *in situ*, which show spectral signatures of atomic hydrogen and atomic oxygen, representing intermediate species that facilitate (and compete with) the conversion of CO_2 to hydrocarbons.

■ ASSOCIATED CONTENT

Supporting Information

The Supporting Information is available free of charge at https://pubs.acs.org/doi/10.1021/acsenergylett.1c01666.

V–*I* characteristic measurements, emission spectrum measurements, gas chromatography (GC) measurements, and liquid ion chromatography (LIC) measurements (PDF)

■ AUTHOR INFORMATION

Corresponding Author

Stephen B. Cronin − *Department of Physics and Astronomy and Ming Hsieh Department of Electrical Engineering, University of Southern California, Los Angeles, California 90089, United States;* orcid.org/0000-0001-9153-7687; Email: scronin@usc.edu

Authors

Sisi Yang − *Department of Physics and Astronomy, University of Southern California, Los Angeles, California 90089, United States;* orcid.org/0000-0003-0352-833X

Bofan Zhao − *Ming Hsieh Department of Electrical Engineering, University of Southern California, Los Angeles, California 90089, United States;* orcid.org/0000-0003-0478-6330

Indu A. Aravind − *Department of Physics and Astronomy, University of Southern California, Los Angeles, California 90089, United States*

Yu Wang − *Mork Family Department of Chemical Engineering and Materials Science, University of Southern California, Los Angeles, California 90089, United States;* orcid.org/0000-0002-0307-1301

Boxin Zhang − *Mork Family Department of Chemical Engineering and Materials Science, University of Southern California, Los Angeles, California 90089, United States*

Sizhe Weng − *Ming Hsieh Department of Electrical Engineering, University of Southern California, Los Angeles, California 90089, United States*

Zhi Cai − *Mork Family Department of Chemical Engineering and Materials Science, University of Southern California, Los Angeles, California 90089, United States*

Ruoxi Li − *Mork Family Department of Chemical Engineering and Materials Science, University of Southern California, Los Angeles, California 90089, United States*

Ali Zarei Baygi − *Sonny Astani Department of Civil and Environmental Engineering, University of Southern California, Los Angeles, California 90089, United States*

Adam Smith − *Sonny Astani Department of Civil and Environmental Engineering, University of Southern California, Los Angeles, California 90089, United States;* orcid.org/0000-0002-3964-7544

Martin A. Gundersen − *Department of Physics and Astronomy and Ming Hsieh Department of Electrical Engineering, University of Southern California, Los Angeles, California 90089, United States*

Complete contact information is available at: https://pubs.acs.org/10.1021/acsenergylett.1c01666

Notes

The authors declare no competing financial interest.

■ ACKNOWLEDGMENTS

This research was supported by the Air Force Office of Scientific Research (AFOSR) Grant No. FA9550-19-1-0115 (S.Y.); Army Research Office (ARO) Award No. W911NF-19-1-0257 (B.Z.); National Science Foundation (NSF) Award Nos. CBET-1905185 (I.A.A.) and CHE-1954834 (R.L.); and U.S. Department of Energy, Office of Basic Energy Sciences Award No. DE-FG02-07ER46376 (Y.W.). Part of this work was carried out using equipment purchased through the Department of Energy Award No. DE-SC0019322.

■ REFERENCES

(1) Hori, Y.; Wakebe, H.; Tsukamoto, T.; Koga, O. Electrocatalytic Process of CO Selectivity in Electrochemical Reduction of CO_2 at Metal Electrodes in Aqueous Media. *Electrochim. Acta* **1994**, *39*, 1833−1839.

(2) Todoroki, M.; Hara, K.; Kudo, A.; Sakata, T. Electrochemical Reduction of High Pressure CO_2 at Pb, Hg and In Electrodes in an Aqueous $KHCO_3$ Solution. *J. Electroanal. Chem.* **1995**, *394*, 199−203.

(3) Hara, K.; Kudo, A.; Sakata, T. Electrochemical Reduction of Carbon Dioxide under High Pressure on Various Electrodes in An aqueous Electrolyte. *J. Electroanal. Chem.* **1995**, *391*, 141−147.

(4) Hori, Y.; Ito, H.; Okano, K.; Nagasu, K.; Sato, S. Silver-coated Ion Exchange Membrane Electrode Applied to Electrochemical Reduction of Carbon Dioxide. *Electrochim. Acta* **2003**, *48*, 2651−2657.

(5) Chaplin, R. P. S.; Wragg, A. A. Effects of Process Conditions and Electrode Material on Reaction Pathways for Carbon Dioxide Electroreduction with Particular Reference to Formate Formation. *J. Appl. Electrochem.* **2003**, *33*, 1107−1123.

(6) Gattrell, M.; Gupta, N.; Co, A. A Review of the Aqueous Electrochemical Reduction of CO_2 to Hydrocarbons at Copper. *J. Electroanal. Chem.* **2006**, *594*, 1−19.

(7) Innocent, B.; Liaigre, D.; Pasquier, D.; Ropital, F.; Leger, J.-M.; Kokoh, K. Electro-reduction of Carbon Dioxide to Formate on Lead Electrode in Aqueous Medium. *J. Appl. Electrochem.* **2009**, *39*, 227−232.

(8) Innocent, B.; Pasquier, D.; Ropital, F.; Hahn, F.; Leger, J.-M.; Kokoh, K. FTIR Spectroscopy Study of the Reduction of Carbon

Dioxide on Lead Electrode in Aqueous Medium. *Appl. Catal., B* **2010**, *94*, 219−224.
(9) Hou, W.; Hung, W. H.; Pavaskar, P.; Goeppert, A.; Aykol, M.; Cronin, S. B. Photocatalytic Conversion of CO_2 to Hydrocarbon Fuels via Plasmon-Enhanced Absorption and Metallic Interband Transitions. *ACS Catal.* **2011**, *1*, 929−936.
(10) Windle, C. D.; Perutz, R. N. Advances in Molecular Photocatalytic and Electrocatalytic CO_2 Reduction. *Coord. Chem. Rev.* **2012**, *256*, 2562−2570.
(11) Zeng, G.; Qiu, J.; Pavaskar, P.; Li, Z.; Cronin, S. B. CO_2 Reduction to Methanol on TiO_2-Passivated GaP Photocatalysts. *ACS Catal.* **2014**, *4*, 3512.
(12) Jones, J.-P.; Prakash, G. K. S.; Olah, G. A. *Isr. J. Chem.* **2014**, *54*, 1451−1466.
(13) Zeng, G.; Qiu, J.; Hou, B.; Shi, H.; Lin, Y.; Hettick, M.; Javey, A.; Cronin, S. B. *Chem. - Eur. J.* **2015**, *21*, 13502−13507.
(14) Qiu, J.; Zeng, G.; Ha, M.-A.; Ge, M.; Lin, Y.; Hettick, M.; Hou, B.; Alexandrova, A. N.; Javey, A.; Cronin, S. B. Artificial Photosynthesis on TiO_2-Passivated InP Nanopillars. *Nano Lett.* **2015**, *15*, 6177−6181.
(15) Zhao, B.; Aravind, I.; Yang, S.; Wang, Y.; Li, R.; Cronin, S. B. Au Nanoparticle Enhancement of Plasma-Driven Methane Conversion into Higher Order Hydrocarbons via Hot Electrons. *ACS Applied Nano Materials* **2020**, *3*, 12388−12393.
(16) Chandrasekaran, K.; Bockris, L. O. M. In-situ spectroscopic investigation of adsorbed intermediate radicals in electrochemical reactions: CO_2^- on platinum. *Surf. Sci.* **1987**, *185*, 495−514.
(17) Bockris, J. O.; Wass, J. C. The Photoelectrocatalytic Reduction of Carbon-Dioxide. *J. Electrochem. Soc.* **1989**, *136*, 2521−2528.
(18) Bockris, J. O.; Wass, J. C. On the Photoelectrocatalytic Reduction of Carbon-Dioxide. *Mater. Chem. Phys.* **1989**, *22*, 249−280.
(19) Eliasson, B.; Liu, C.-j.; Kogelschatz, U. Direct Conversion of Methane and Carbon Dioxide to Higher Hydrocarbons Using Catalytic Dielectric-Barrier Discharges with Zeolites. *Ind. Eng. Chem. Res.* **2000**, *39*, 1221−1227.
(20) Paulussen, S.; Verheyde, B.; Tu, X.; De Bie, C.; Martens, T.; Petrovic, D.; Bogaerts, A.; Sels, B. Conversion of Carbon Dioxide to Value-added Chemicals in Atmospheric Pressure Dielectric Barrier Discharges. *Plasma Sources Sci. Technol.* **2010**, *19*, 034015.
(21) Aerts, R.; Somers, W.; Bogaerts, A. *ChemSusChem* **2015**, *8*, 702−716.
(22) Tsuji, M.; Tanoue, T.; Nakano, K.; Nishimura, Y. Decomposition of CO_2 into CO and O in a Microwave-Excited Discharge Flow of CO_2/He or CO_2/Ar Mixtures. *Chem. Lett.* **2001**, *30*, 22−23.
(23) Heijkers, S.; Snoeckx, R.; Kozák, T.; Silva, T.; Godfroid, T.; Britun, N.; Snyders, R.; Bogaerts, A. CO_2 Conversion in a Microwave Plasma Reactor in the Presence of N_2: Elucidating the Role of Vibrational Levels. *J. Phys. Chem. C* **2015**, *119*, 12815−12828.
(24) Mitsingas, C. M.; Rajasegar, R.; Hammack, S.; Do, H.; Lee, T. High Energy Efficiency Plasma Conversion of CO_2 at Atmospheric Pressure Using a Direct-Coupled Microwave Plasma System. *IEEE Trans. Plasma Sci.* **2016**, *44*, 651−656.
(25) Malik, M. A.; Jiang, X. Z. The CO_2 Reforming of Natural Gas in a Pulsed Corona Discharge Reactor. *Plasma Chem. Plasma Process.* **1999**, *19*, 505−512.
(26) Wen, Y.; Jiang, X. Decomposition of CO_2 Using Pulsed Corona Discharges Combined with Catalyst. *Plasma Chem. Plasma Process.* **2001**, *21*, 665−678.
(27) Scapinello, M.; Martini, L. M.; Dilecce, G.; Tosi, P. Conversion of CH_4/CO_2 by a Nanosecond Repetitively Pulsed Discharge. *J. Phys. D: Appl. Phys.* **2016**, *49*, 075602.
(28) Liu, J.-L.; Park, H.-W.; Chung, W.-J.; Ahn, W.-S.; Park, D.-W. Simulated Biogas Oxidative Reforming in AC-pulsed Gliding Arc Discharge. *Chem. Eng. J.* **2016**, *285*, 243−251.
(29) Istadi; Amin, N. A. S. Co-generation of Synthesis Gas and C_{2+} Hydrocarbons from Methane and Carbon Dioxide in a Hybrid Catalytic-Plasma Reactor: A Review. *Fuel* **2006**, *85*, 577−592.
(30) Ashford, B.; Tu, X. Non-thermal Plasma Technology for the Conversion of CO_2. *Current Opinion in Green and Sustainable Chemistry* **2017**, *3*, 45−49.
(31) Bogaerts, A.; De Bie, C.; Snoeckx, R.; Kozák, T. *Plasma Processes Polym.* **2017**, *14*, 1600070.
(32) Snoeckx, R.; Wang, W.; Zhang, X.; Cha, M. S.; Bogaerts, A. Plasma-based Multi-reforming for Gas-To-Liquid: Tuning the Plasma Chemistry towards Methanol. *Sci. Rep.* **2018**, *8*, 15929.
(33) Snoeckx, R.; Ozkan, A.; Reniers, F.; Bogaerts, A. The Quest for Value-Added Products from Carbon Dioxide and Water in a Dielectric Barrier Discharge: A Chemical Kinetics Study. *ChemSusChem* **2017**, *10*, 409−424.
(34) Chen, G.; Godfroid, T.; Britun, N.; Georgieva, V.; Delplancke-Ogletree, M.-P.; Snyders, R. Plasma-catalytic conversion of CO2 and CO2/H2O in a surface-wave sustained microwave discharge. *Appl. Catal., B* **2017**, *214*, 114−125.
(35) Yao, X.; Zhang, Y.; Wei, Z.; Chen, M.; Shangguan, W. Plasma-Catalytic Conversion of CO2 and H2O into H2, CO, and Traces of CH4 over NiO/Cordierite Catalysts. *Ind. Eng. Chem. Res.* **2020**, *59*, 19133−19144.
(36) Rumbach, P.; Xu, R.; Go, D. B. Electrochemical Production of Oxalate and Formate from CO2 by Solvated Electrons Produced Using an Atmospheric-Pressure Plasma. *J. Electrochem. Soc.* **2016**, *163*, F1157−F1161.
(37) Clements, J. S.; Sato, M.; Davis, R. H. Preliminary Investigation of Prebreakdown Phenomena and Chemical Reactions Using a Pulsed High-Voltage Discharge in Water. *IEEE Trans. Ind. Appl.* **1987**, *IA-23*, 224−235.
(38) Sunka, P. Pulse Electrical Discharges in Water and their Applications. *Phys. Plasmas* **2001**, *8*, 2587−2594.
(39) Lu, X.; Pan, Y.; Liu, K.; Liu, M.; Zhang, H. *J. Appl. Phys.* **2002**, *91*, 24−31.
(40) Miichi, T.; Hayashi, N.; Ihara, S.; Satoh, S.; Yamabe, C. Generation of Radicals using Discharge inside Bubbles in Water for Water Treatment. *Ozone: Sci. Eng.* **2002**, *24*, 471−477.
(41) Yamabe, C.; Takeshita, F.; Miichi, T.; Hayashi, N.; Ihara, S. Water Treatment Using Discharge on the Surface of a Bubble in Water. *Plasma Processes Polym.* **2005**, *2*, 246−251.
(42) Sahni, M.; Locke, B. R. Quantification of Hydroxyl Radicals Produced in Aqueous Phase Pulsed Electrical Discharge Reactors. *Ind. Eng. Chem. Res.* **2006**, *45*, 5819−5825.
(43) Lukes, P.; Clupek, M.; Babicky, V.; Sunka, P. Pulsed Electrical Discharge in Water Generated Using Porous-Ceramic-Coated Electrodes. *IEEE Trans. Plasma Sci.* **2008**, *36*, 1146−1147.
(44) Sato, M. Environmental and Biotechnological Applications of High-voltage Pulsed Discharges in Water. *Plasma Sources Sci. Technol.* **2008**, *17*, 024021.
(45) Dong, F.; Zhang, J.; Wang, K.; Liu, Z.; Guo, J.; Zhang, J. Cold Plasma Gas Loaded Microbubbles as a Novel Ultrasound Contrast Agent. *Nanoscale* **2019**, *11*, 1123−1130.
(46) Zhao, B.; Aravind, I.; Yang, S.; Cai, Z.; Wang, Y.; Li, R.; Subramanian, S.; Ford, P.; Singleton, D. R.; Gundersen, M. A.; Cronin, S. B. Nanoparticle-Enhanced Plasma Discharge Using Nanosecond High-Voltage Pulses. *J. Phys. Chem. C* **2020**, *124*, 7487−7491.
(47) Zhao, B.; Aravind, I.; Yang, S.; Wang, Y.; Li, R.; Zhang, B.; Wang, Y.; Dawlaty, J. M.; Cronin, S. B. Enhanced Plasma Generation from Metal Nanostructures via Photoexcited Hot Electrons. *J. Phys. Chem. C* **2021**, *125*, 6800−6804.
(48) Dean, J. A.; Lange, N.A. *Lange's Handbook of Chemistry*, 15th ed.; McGraw-Hill, 1999.
(49) Enick, R. M.; Klara, S. M. CO_2 Solubility in Water and Brine under Reservoir Conditions. *Chem. Eng. Commun.* **1990**, *90*, 23−33.
(50) Portier, S.; Rochelle, C. Modelling CO2 solubility in pure water and NaCl-type waters from 0 to 300 degrees C and from 1 to 300 bar - Application to the Utsira Formation at Sleipner. *Chem. Geol.* **2005**, *217*, 187−199.
(51) Caumon, M. C.; Sterpenich, J.; Randi, A.; Pironon, J. Measuring mutual solubility in the H2O-CO2 system up to 200 bar

https://doi.org/10.1021/acsenergylett.1c01666
ACS Energy Lett. 2021, 6, 3924−3930

and 100 degrees C by in situ Raman spectroscopy. *Int. J. Greenhouse Gas Control* **2016**, *47*, 63−70.
(52) Duan, Z.; Sun, R. An improved model calculating CO2 solubility in pure water and aqueous NaCl solutions from 273 to 533 K and from 0 to 2000 bar. *Chem. Geol.* **2003**, *193*, 257−271.
(53) Zhang, D.; Huang, Q.; Devid, E. J.; Schuler, E.; Shiju, N. R.; Rothenberg, G.; van Rooij, G.; Yang, R.; Liu, K.; Kleyn, A. W. Tuning of Conversion and Optical Emission by Electron Temperature in Inductively Coupled CO2 Plasma. *J. Phys. Chem. C* **2018**, *122*, 19338−19347.
(54) Spencer, L.; Gallimore, A. Investigation of Atmospheric Pressure Plasma Source for CO_2 Dissociation; **2011**.
(55) Ling, H.; Shen, X.; Han, Y.; Lu, Y. Investigation of CO_2 gas breakdown using optical emission spectroscopy. *Proc. SPIE* **2006**, *6107*, 61070A.
(56) Motret, O.; Pellerin, S.; Nikravech, M.; Massereau, V.; Pouvesle, J. M. Spectroscopic Characterization of CH4 + CO2 Plasmas Excited by a Dielectric Barrier Discharge at Atmospheric Pressure. *Plasma Chem. Plasma Process.* **1997**, *17*, 393−407.
(57) Le Quang, D.; Babou, Y.; Andre, P. Investigations of a microwave plasma source operating with air, N2, CO2and argon gases. *IOP Conf. Ser.: Mater. Sci. Eng.* **2012**, *29*, 012009.
(58) Zeng, Y.; Tu, X. Plasma-Catalytic CO_2 Hydrogenation at Low Temperatures. *IEEE Trans. Plasma Sci.* **2016**, *44*, 405−411.
(59) Nicholls, R. W. The Interpretation of Intensity Distributions in the CN Violet, C_2 Swan, OH Violet and O_2 Schumann-Runge Band Systems by use of theirr-Centroids and Franck-Condon Factors. *Proc. Phys. Soc., London, Sect. A* **1956**, *69*, 741−753.
(60) Billoux, T.; Cressault, Y.; Boretskij, V. F.; Veklich, A. N.; Gleizes, A. Net emission coefficient of CO2-Cu thermal plasmas: role of copper and molecules. *J. Phys.: Conf. Ser.* **2012**, *406*, 012027.
(61) Hori, Y.; Kikuchi, K.; Murata, A.; Suzuki, S. *Chem. Lett.* **1986**, *15*, 897−898.
(62) Garza, A. J.; Bell, A. T.; Head-Gordon, M. Mechanism of CO2 Reduction at Copper Surfaces: Pathways to C2 Products. *ACS Catal.* **2018**, *8*, 1490−1499.
(63) Raciti, D.; Wang, C. Recent Advances in CO2 Reduction Electrocatalysis on Copper. *ACS Energy Letters* **2018**, *3*, 1545−1556.
(64) Joshi, A. A.; Locke, B. R.; Arce, P.; Finney, W. C. Formation of Hydroxyl Radicals, Hydrogen Peroxide and Aqueous Electrons by Pulsed Streamer Corona Discharge in Aqueous Solution. *J. Hazard. Mater.* **1995**, *41*, 3−30.
(65) Sato, M.; Ohgiyama, T.; Clements, J. S. Formation of Chemical Species and Their Effects on Microorganisms using a Pulsed High-voltage Discharge in Water. *IEEE Trans. Ind. Appl.* **1996**, *32*, 106−112.
(66) Sunka, P.; Babický, V.; Clupek, M.; Lukes, P.; Simek, M.; Schmidt, J.; Cernak, M. Generation of Chemically Active Species by Electrical Discharges in Water. *Plasma Sources Sci. Technol.* **1999**, *8*, 258.
(67) Grymonpré, D. R.; Sharma, A. K.; Finney, W. C.; Locke, B. R. The Role of Fenton's Reaction in Aqueous Phase Pulsed Streamer Corona Reactors. *Chem. Eng. J.* **2001**, *82*, 189−207.
(68) Koprivanac, N.; Kušić, H.; Vujević, D.; Peternel, I.; Locke, B. R. Influence of Iron on Degradation of Organic Dyes in Corona. *J. Hazard. Mater.* **2005**, *117*, 113−119.
(69) Pekker, M.; Seepersad, Y.; Shneider, M. N.; Fridman, A.; Dobrynin, D. Initiation Stage of Nnosecond Breakdown in Liquid. *J. Phys. D: Appl. Phys.* **2014**, *47*, 025502.
(70) Zhang, L.; Zhu, D.; Nathanson, G. M.; Hamers, R. J. Selective Photoelectrochemical Reduction of Aqueous CO_2 to CO by Solvated Electrons. *Angew. Chem., Int. Ed.* **2014**, *53*, 9746−9750.
(71) Rumbach, P.; Bartels, D. M.; Sankaran, R. M.; Go, D. B. The Solvation of Electrons by An Atmospheric-pressure Plasma. *Nat. Commun.* **2015**, *6*, 7248.
(72) Neta, P.; Simic, M.; Hayon, E. Pulse radiolysis of aliphatic acids in aqueous solutions. I. Simple monocarboxylic acids. *J. Phys. Chem.* **1969**, *73*, 4207−4213.
(73) Getoff, N. Possibilities on the radiation-induced incorporation of CO2 and CO into organic compounds. *Int. J. Hydrogen Energy* **1994**, *19*, 667−672.
(74) Flyunt, R.; Schuchmann, M. N.; von Sonntag, C. A common carbanion intermediate in the recombination and proton-catalysed disproportionation of the carboxyl radical anion, CO2*-, in aqueous solution. *Chem. - Eur. J.* **2001**, *7*, 796−9.
(75) Mota-Lima, A. The Electrified Plasma/Liquid Interface as a Platform for Highly Efficient CO2 Electroreduction to Oxalate. *J. Phys. Chem. C* **2020**, *124*, 10907−10915.
(76) Zhu, D.; Zhang, L.; Ruther, R. E.; Hamers, R. J. Photo-illuminated Diamond as A Solid-state Source of Solvated Electrons in Water for Nitrogen Reduction. *Nat. Mater.* **2013**, *12*, 836.
(77) Hawtof, R.; Ghosh, S.; Guarr, E.; Xu, C.; Mohan Sankaran, R.; Renner, J. N. Catalyst-free, Highly Selective Synthesis of Ammonia from Nitrogen and Water by A Plasma Electrolytic System. *Science Advances* **2019**, *5*, No. eaat5778.
(78) Genovese, C.; Ampelli, C.; Perathoner, S.; Centi, G. Mechanism of C-C bond formation in the electrocatalytic reduction of CO2 to acetic acid. A challenging reaction to use renewable energy with chemistry. *Green Chem.* **2017**, *19*, 2406−2415.
(79) Bogaerts, A.; Kozák, T.; van Laer, K.; Snoeckx, R. Plasma-based conversion of CO2: current status and future challenges. *Faraday Discuss.* **2015**, *183*, 217−232.
(80) Yang, S.; Ford, P.; Subramanian, S.; Singleton, D.; Sanders, J.; Cronin, S. B. Transient Plasma-enhanced Remediation of Nanoscale Particulate Matter in Restaurant Smoke Emissions via Electrostatic Precipitation. *Particuology* **2021**, *55*, 43−47.
(81) Yang, S.; Subramanian, S.; Singleton, D.; Schroeder, C.; Schroeder, W.; Gundersen, M. A.; Cronin, S. B. First Results on Transient Plasma-based Remediation of Nanoscale Particulate Matter in Restaurant Smoke Emissions. *Environ. Res.* **2019**, *178*, 108635.
(82) Schroeder, C.; Schroeder, W.; Yang, S.; Nystrom, A.; Cai, Z.; Subramanian, S.; Li, S.; Gundersen, M. A.; Cronin, S. B. Plasma-enhanced NOx remediation using nanosecond pulsed discharges in a water aerosol matrix. *Fuel Process. Technol.* **2020**, *208*, 106521.
(83) Schroeder, C.; Schroeder, W.; Yang, S.; Shi, H.; Nystrom, A.; Subramanian, S.; Li, S.; Gundersen, M. A.; Cronin, S. B. Plasma-enhanced SO2 Remediation in A Humidified Gas Matrix: A Potential Strategy for the Continued Burning of High Sulfur Bunker Fuel. *Fuel* **2020**, *274*, 117810.

https://doi.org/10.1021/acsenergylett.1c01666
ACS Energy Lett. 2021, 6, 3924−3930